

EFFECTS OF FEED RATE AND RESIDENCE TIME ON ENVIRONMENT OF ROTARY DRYER PROCESSES

MARGONO, M.TAUFIK H., ALI ALYWAY*, KUSWANDI and SUSIANTO

Heat & Mass Transfer Laboratory, Department of Chemical Engineering, Sepuluh Nopember Institute of Technology, Campus ITS Surabaya 60111, Indonesia.

*Corresponding Author: Phone: +6281931075670, E-mail: alimohad@chem-eng.its.ac.id

Received: 26th December 2008; Revised: 12th February 2009; Accepted: 14th February 2009

Abstract: The aim of this work was to analyze the effects of feed rate and residence time in rotary dryer using steady-state and unsteady-state plug flow models. Partial differential equations describing heat and mass transfer in the rotary dryer were derived from shell balance. Analytical methods were used to solve these partial differential equations using Matlab facility. Some dimensionless groups are used and came up with dimensionless equations. Validation of the computation results was carried out using the pilot rotary dryer data of a fertilizer factory. The computation results were also compared with the experimental data. The results revealed that evaporated ammonium sulphate's moisture content in Plug Flow Back Mixing model was lower than in Plug Flow model. More than 5 % rate of dusting could be occurred in rotary dryer processes and rate of dusting depends upon feed rate and residence time.

Keywords: Rotary dryer, plug flow, rate of dusting, environment

INTRODUCTION

Dusting in a rotary dryer was an important factor to limit the amount of air for drying materials. The amount of dust in a rotary dryer processing increased along with drying air velocity and depended on the slope of the dryer. The allowable amount of dust in a rotary dryer was 5 % to keep uncontaminated environment of the dryer. Usually materials in rotary dryer are flied to the higher part of the rotary dryer by the effects of the flights and then fall to the lower parts, and back mixing of the solid is occurred (Fig. 1). Previous workers have used experiment to get heat transfer coefficient and operation variables effects in drying process and confirmed the heat transfer test [1]. Modelling of drying process in rotary dryer for a certain material was developed by some researchers [2-4]. They developed model and assumed rotary dryer as a plug-flow reactor. A special solid axial dispersion in rotary dryer was found [5]. Granule could be transported at steady-state in a horizontal rotary drum with inclined flights. However, heat

transfer and mass transfer with axial solid dispersion simulation research were not available. Heat and mass transfer phenomena in the rotary dryer should be studied well in order to analyze and to design rotary dryer. Therefore, mathematical model and simulation in rotary dryer was the concern of this research. Drying phenomena will be useful in design process and determining optimum rotary dryer conditions. The aim of this work was to analyze the effects of parameters on environment of rotary dryer, such as feed rate or rate of drying air and residence time in rotary dryer using steady-state and unsteady-state plug flow models.

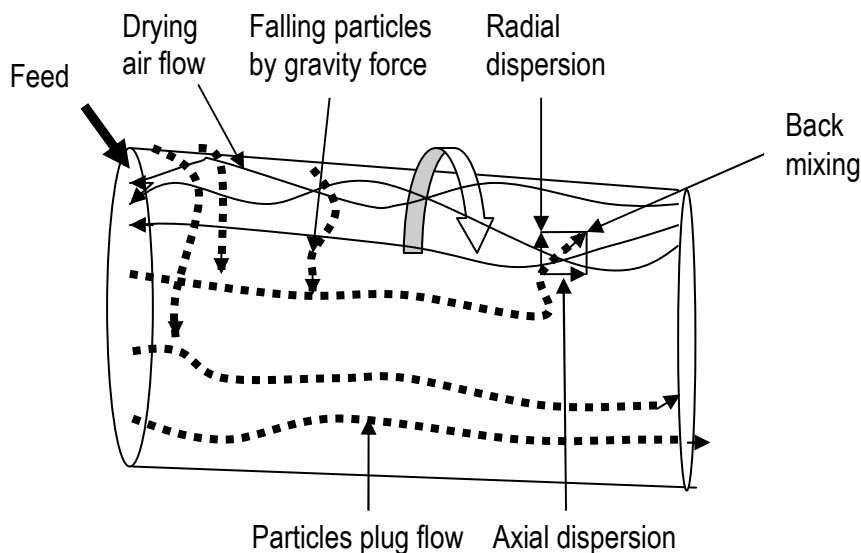


Fig. 1: Flows in a rotary dryer

MATERIALS AND METHODS

Drying in rotary dryer has been used widely in industries, because it produces good mass and heat transfer properties. A rotary dryer consist of rotating cylinder which has an angle to the horizontal where input material from one end and output product from the other end. Dry air was used as a drying media. A rotary dryer was used in this work with 12.2 m length, 2.418 m diameter, 4.5 % slope and 3.5 rpm and ammonium sulphate feed.

Experiment and simulation were used in this work. Tray dryer was used in this experimental method to find the drying rate of the solid. The result of rotary dryer's model was a system differential equation which could be solved analytically by separation variables method. Steady-state and unsteady state mass transfer conditions as well as solid and air dryer's moisture content were used as a model approach. Volumetric heat transfer coefficient and residence time were estimated [1, 6] as presented in equation (1) and (2)

$$U_v = \frac{k_1 G^{0.67}}{D} \quad (1)$$

$$\frac{-}{\tau} = \frac{k_2 H^*}{W} \quad (2)$$

Where G = air mass rate ($\text{kg s}^{-1}\text{m}^{-2}$), D = rotary dryer diameter (m), k_1 = constant value ranging from 0.3 to 0.5, k_2 = constant value ranging from 0.8 to 0.9, H^* = holdup (kg), $\bar{\tau}$ = average time of passage (s), U_v = heat transfer volumetric coefficient ($\text{kJ m}^{-3}\cdot\text{K}^{-1}\cdot\text{s}^{-1}$), W = feed rate (kg s^{-1}).

Steady-state plug flow modelling can be developed from shell mass balance of system as described in Figure 2.

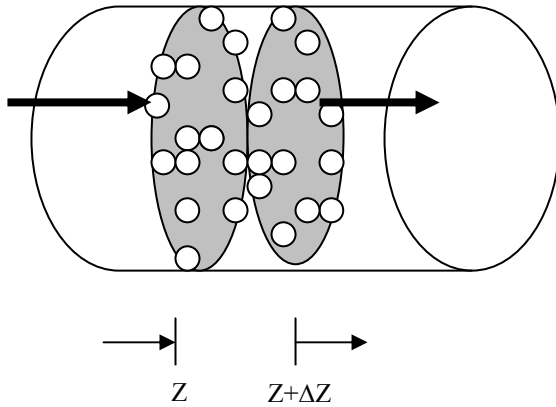


Fig. 2: Cross sectional area mass balance in a rotary dryer.

The shell mass balance could be written as follows: Mass convection input rate – Mass convection output rate + Mass evaporation rate = Mass accumulation rate. Then it arrived in steady-state equation as follows:

$$V_s \frac{\partial X}{\partial z} = -R_w \quad (3)$$

Where L = dryer length (m), R_w = drying rate (1 s^{-1}), V_s = solid linear rate in axial direction (m s^{-1}), X = mass of moisture per solid mass (-), z = axial distant (m).

Using boundary conditions:

$$\text{BC 1 at } z = 0, \quad X = X_0 \quad (4)$$

and dimensionless group

$$F = \frac{X}{X_0} \rightarrow X_0 \partial F = \partial X$$

$$\xi = \frac{z}{L} \rightarrow L \partial \xi = \partial z$$

$$\phi = \frac{R_w L}{V_s X_0} \rightarrow R_w = \frac{V_s X_0}{L} \phi$$

Where F = dimensionless moisture content, ξ = dimensionless length, $\phi = \frac{R_w L}{V_s X_0}$ = a constant.

Substitution these dimensionless groups into equation (3), it follows:

$$V_s \frac{X_0 \partial F}{L \partial \xi} = - \frac{V_s X_0}{L} \phi$$

$$\frac{\partial F}{\partial \xi} = -\phi \quad (5)$$

$$\int_1^F \partial F = -\phi \int_0^\xi \partial \xi$$

$$F = 1 - \phi \xi \quad (6)$$

For non steady-state plug flow modelling by mass balance calculation on a cylindrical shell, the following equation was obtained:

$$\frac{\partial X}{\partial t} + V_s \frac{\partial X}{\partial z} = -R_w \quad (7)$$

Where t = time (hour)

Boundary and initial conditions for partial differential equation were described in equation (8) through (10).

$$\text{BC 1 at } z = 0, X = X_0 \quad (8)$$

$$\text{BC 2 at } z = L, X = \text{finite} \quad (9)$$

$$\text{IC at } t = 0, X = X_0 \quad (10)$$

Analytical solution of equation (7) with their boundaries could be described as follows:

First we define dimensionless groups

$$F = \frac{X}{X_0} \rightarrow X_0 \partial F = \partial X; \quad \theta = t \frac{V_s}{L} \rightarrow \frac{L}{V_s} \partial \theta = \partial t$$

$$\xi = \frac{z}{L} \rightarrow L \partial \xi = \partial z; \quad \phi = \frac{R_w L}{V_s X_0} \rightarrow R_w = \frac{V_s X_0}{L} \phi \quad \text{Where } \theta = \text{dimensionless time.}$$

The dimensionless groups were combined with equation (7), and then an equation with three variables was obtained.

$$\frac{\partial F}{\partial \theta} + \frac{\partial F}{\partial \xi} = -\phi \quad (11)$$

$$\frac{\partial F}{\partial \xi} = -\frac{\partial F}{\partial \theta} - \phi = -\lambda^2$$

$$\frac{\partial F}{\partial \xi} = -\lambda^2$$

$$F = 1 - \lambda^2 \xi$$

$$\lambda^2 = \frac{1-F}{\xi}$$

$$\frac{\partial F}{\partial \theta} + \phi = \lambda^2$$

Solving the equations, then it found

$$F = 1 - \frac{\phi \theta}{1 + \frac{\theta}{\xi}} \quad (12)$$

Steady-state plug flow modelling with back mixing was obtained from the mass balance in cylindrical shell, and then an equation was obtained.

$$V_s \frac{\partial X}{\partial z} + D_z \frac{\partial^2 X}{\partial z^2} = -R_w \quad (13)$$

Where D_z = axial dispersion coefficient ($m^2 h^{-1}$)

Boundary conditions:

$$\text{BC 1 at } z = 0, \text{ then } X = X_0 \quad (14)$$

$$\text{BC 2 at } z = L, \text{ then } X = \text{finite} \quad (15)$$

The following dimensionless groups were defined:

$$F = \frac{X}{X_0} \rightarrow X_0 \partial F = \partial X$$

$$\xi = \frac{z}{L} \rightarrow L \partial \xi = \partial z$$

$$\phi = \frac{R_w L}{V_s X_0} \rightarrow R_w = \frac{V_s X_0}{L} \phi$$

$$P_e = \frac{LV_s}{D_z} \rightarrow D_z = \frac{LV_s}{P_e}$$

$$\text{Where } P_e = \frac{LV_s}{D_z} = \text{Pecllet number} \quad (16)$$

The dimensionless groups were substituted into equation (13)

$$V_s \frac{X_0 \partial F}{L \partial \xi} + \frac{LV_s}{P_e} \frac{X_0 \partial^2 F}{L^2 \partial \xi^2} = -\frac{V_s X_0}{L} \phi \quad (17)$$

$$\frac{\partial F}{\partial \xi} + \frac{1}{P_e} \frac{\partial^2 F}{\partial \xi^2} = -\phi \quad \text{By substitution } p = \frac{\partial F}{\partial \xi} \text{ into equation (17) we obtained equation (18)}$$

$$p + \frac{1}{P_e} \frac{\partial p}{\partial \xi} = -\phi \quad (18)$$

$$\frac{\partial p}{\partial \xi} = -(\phi + p)P_e$$

$$\int_0^p \frac{\partial p}{(\phi + p)} = -\int_0^\xi P_e \partial \xi \quad \longrightarrow \quad \ln\left(\frac{p + \phi}{\phi}\right) = -P_e \xi$$

$$p = \phi \exp.(-P_e \xi) - \phi \quad (19)$$

From equation (19), the following equation was formed:

$$\int_1^F \partial F = \int_0^\xi \phi \exp.(-P_e \xi) \partial \xi - \int_0^\xi \phi \partial \xi$$

$$F = 1 - \frac{\phi}{P_e} \exp.(-P_e \xi) + \frac{\phi}{P_e} - \phi \xi \quad (20)$$

RESULTS AND DISCUSSION

Computational works

The computational results obtained from this study showed the rotary dryer performance under steady-state and unsteady-state conditions and using plug flow and plug flow with back mixing modelling. Figure 3 presented a plot between moisture content versus dryer length in a non-steady state plug flow modelling. In 30 seconds, outlet moisture content in solid was 0.75 %, while in 949.8 seconds, output moisture content was 0,138 %. Figure 4 presented a plot of moisture content versus drying time in a non steady-state plug flow modelling, at several point in the rotary dryer. Moisture content in the solid will change significantly in 300 seconds and cotinuously increase until 949.8 s where finally it reached 0,138 %. It would be better using rotary dryer time process more than 949.8 seconds to get solid moisture content product lower than 0.138 %. It was concluded that moisture content in solid particles was more than 0.1 % during 949.8 seconds.

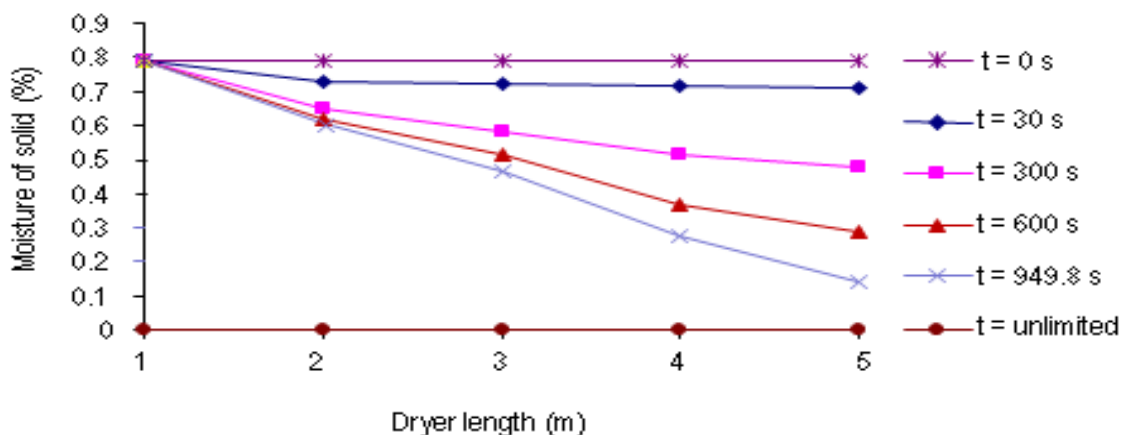


Fig. 3: Moisture of solid (%) and dryer length

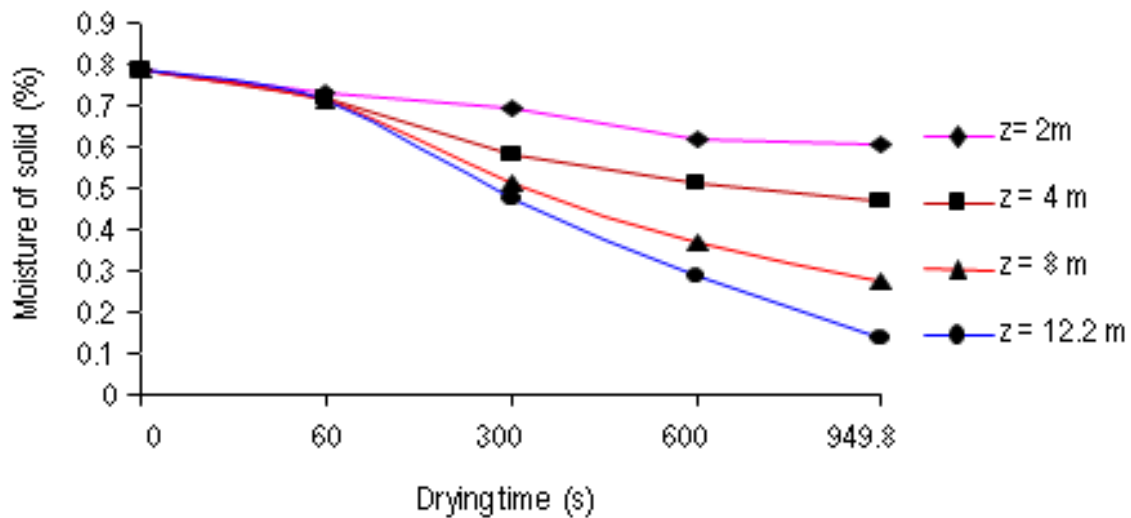


Fig. 4: Moisture of solid and drying time

Figure 5 is a plot of dimensionless moisture content versus dryer length, describing the steady-state (SS) and non steady-state (Non SS) plug flow modelling. Using steady-state plug flow modelling, it would be approached a non steady-state plug flow values in 600 seconds, while in 949.8 seconds (fertilizer's factory time in pilot data of rotary dryer processes) non steady-state plug flow modelling was better than steady-state plug flow modelling. The computational results of non steady-state plug flow modelling as seen in equation (7) was described by moisture content in a solid as function of axial distant and time. Figure 6 presented a plot of dimensionless moisture content versus dimensionless dryer length, where steady-state and non steady-state plug flow modelling was compared. We could conclude that a rotary dryer's developed model based on heat and mass transfer was needed to recover this deviation by using some rotary dryer's parameters model in industrial processes.

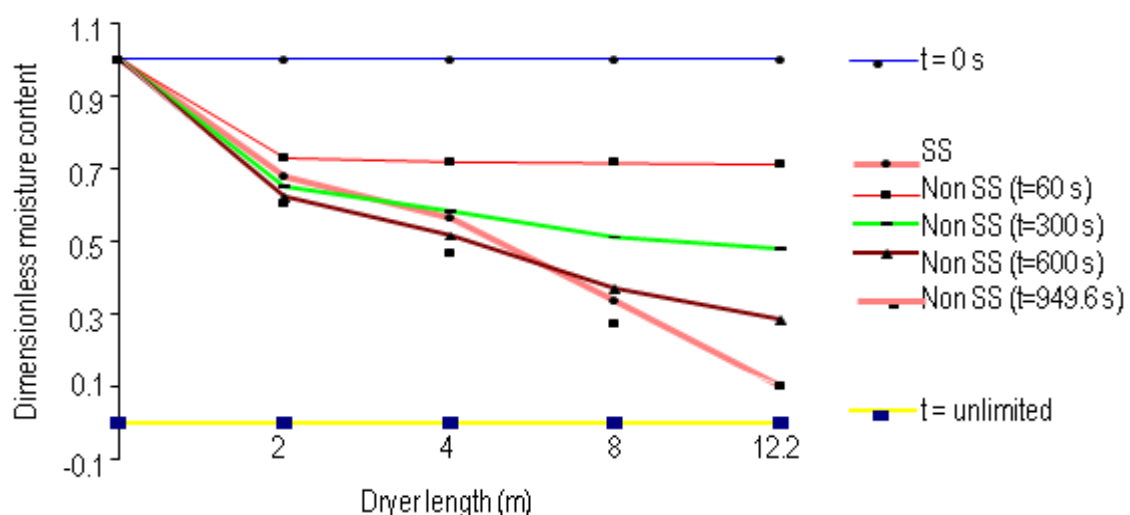


Fig. 5: Dimensionless moisture content and dryer length in steady state and non-steady state modelling

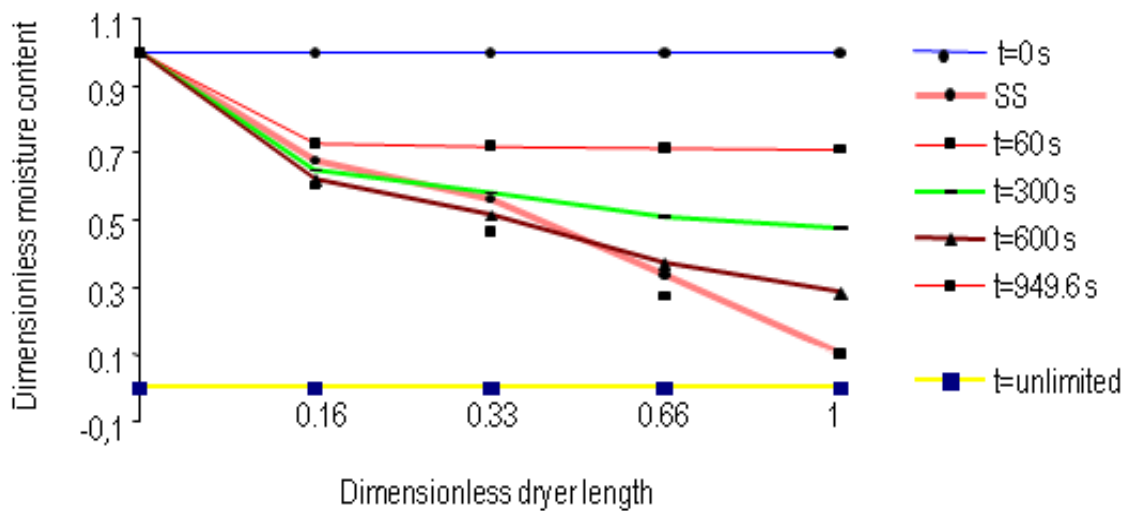


Fig. 6: Dimensionless moisture content and dimensionless dryer length

Effects of ammonium sulfate's feed rate

Figure 7 presented plot of moisture content (%) versus rotary dryer dimensionless length. High feed rate and low feed rate processes are plotted in Fig. 7(a) and (b) respectively. It could be concluded that at high feed rate (32,000 kg h⁻¹), moisture content of ammonium sulfate rotary dryer's outlet is higher than at lower feed rate (22,000 kg h⁻¹), but the increased is not significant. For example, if ammonium sulphate feed rate increased by 45 %, than increasing outlet ammonium sulfate's moisture content only 0.02 %. It was concluded that the second feed rate was better than the first one, because dusting effects on environment were acceptable. The amount of dusting increased slightly with increasing feed rate.

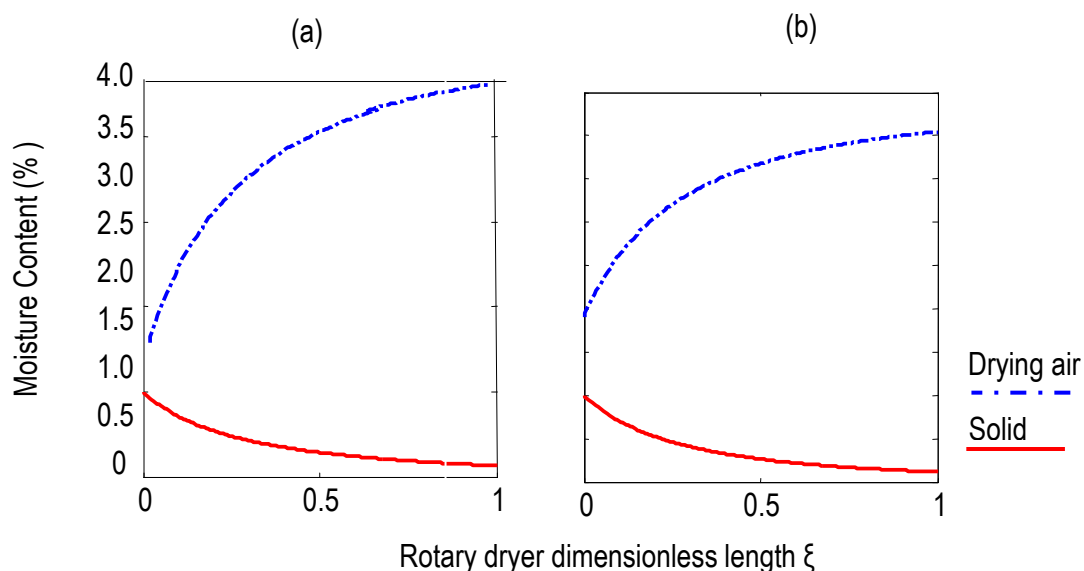


Fig. 7: Profile of solid moisture content (X), air dryer's moisture content (Y) and dimensionless length of rotary dryer ξ for high feed rate (a) and low feed rate (b)

Effects of drying air flow rate

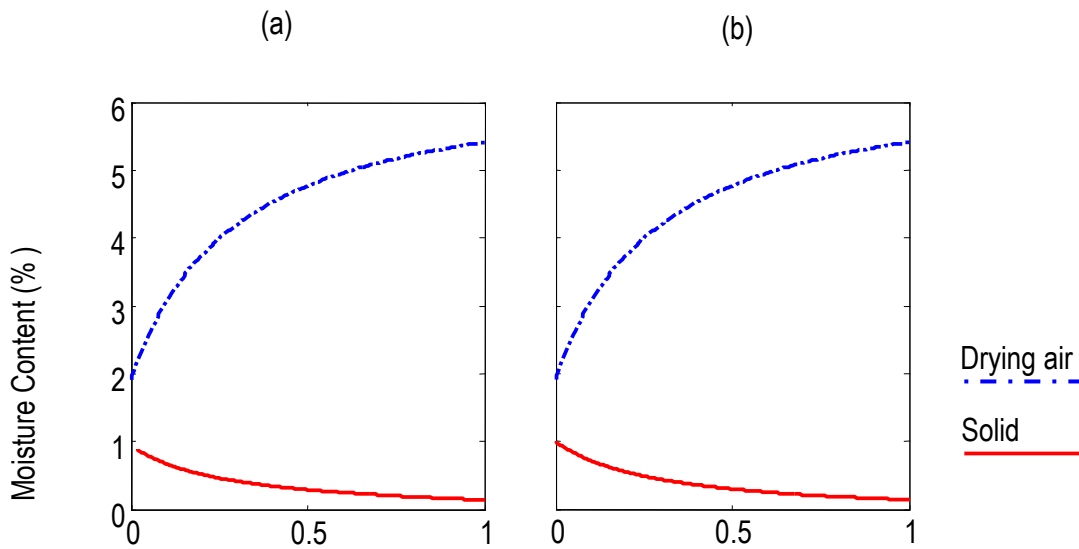


Fig. 8: Profile of solid moisture content (X), air dryer’s moisture content (Y) and dimensionless length of rotary dryer ξ for high (a) and low drying air flow rate (b)

The different between evaporated ammonium sulfate’s moisture content in a high air dryer rate ($12,000 \text{ m}^3 \text{ h}^{-1}$) and a low air dryer rate ($7,000 \text{ m}^3 \text{ h}^{-1}$) was not significant. In Figure 8, if air dryer rate increased by 71 %, than increasing ammonium sulphate’s moisture content only 3 %. Effect of drying air on dusting was plotted in Fig 9 and in Table1.

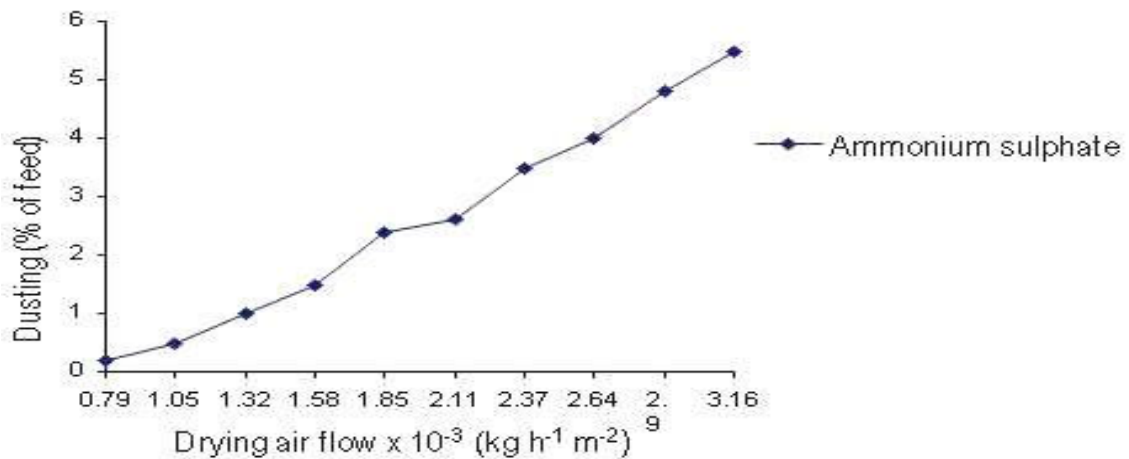


Fig. 9: Dusting and drying air flow

Dusting of ammonium sulphate increased with feed rate of air flow (Table 1). Figure 9 was a plot of dusting versus drying air flow. If material feed rate $22,000 \text{ kg h}^{-1}$ then we have dusting rate of 44 to 1210 kg h^{-1} . When ammonium sulphate feed rate of $32,000 \text{ kg h}^{-1}$, then dusting rate of 64 to 1760 kg h^{-1} were occurred. Environment of rotary dryer was polluted by this process.

Cyclone usually equipped to rotary dryer to collect dusting and also flow of drying air control is needed. This experiment reported that effect of modelling on dusting was not significant.

Table1: Effects of drying air on dusting (% of feed)

Flow of drying air		Dusting
m ³ h ⁻¹	kg h ⁻¹ m ⁻²	% of feed
3000	790.85	0.2
4000	1054.47	0.5
5000	1318.08	1.0
6000	1581.70	1.5
7000	1845.32	2.4
8000	2108.93	2.6
9000	2372.55	3.5
10000	2636.17	4.0
11000	2899.78	4.8
12000	3163.40	5.5

CONCLUSION

The current research found that the increasing rate of dusting of more than 500 kg h⁻¹ did not decrease moisture content significantly. Increasing air rate of 71 % resulted in increasing ammonium sulphate's moisture content of 3 %. Feed rate and residence time affected dusting rate.

Acknowledgment: This work was supported by Department of Chemical Engineering, Faculty of Industrial Technology, Surabaya Sepuluh Nopember Institute of Technology (ITS).The authors also would like to thank to Petro Kimia fertilizer factory, for their facility support.

References

1. Friedman, S.J.and W.R. Marshall Jr, 1949. Studies in Rotary Drying - Part 1. Holdup and Dusting. *Chemical Engineering Progress*, 45 (8): 482-493.
2. Wang, F.Y., I.T. Cameron, J.D. Litster and P.L. Douglas, 1993. A Distributed Parameter Approach to the Dynamics of Rotary Drying Processes. *Drying Technolog*, 11(7): 1641-1656.
3. Pacheco, R.F. and S.S. Stella,1998. Calculating Capacity Trend in Rotary Dryer. *Brazilian Journal of Chemical Engineering*,15 (3): 201-214.
4. Yliniemi, L., 1999. Advanced Control of a Rotary Dryer. PhD Thesis, Department of Process Engineering, University of Oulu, Finland.
5. Pan, J.P.,T.J. Wang, J.J. Yao and Y. Jin, 2006. Granule transport and mean residence time in horizontal drum with inclined flights. *Powder Technology*, 16: 50–58.
6. Lisboa, M.H., A.B. Alves, D.S. Vitorino, W.B.Delaiba, J.R.D.Finzer, and M.A.S.Barrozo, 2007. A study of particle motion in rotary dryers. *Brazilian Journal of Chemical Engineering*. 24(03): 365 – 374.